A model of stressed liquid crystals: close-packed, shaped liquid crystal droplets inside a sheared polymer matrix

Guoqiang Zhang, Anatoliy Glushchenko, John L. West*, Ivan Smalyukh, Oleg Lavrentovich

Liquid Crystal Institute, Kent State University, Kent, OH 44242

ABSTRACT

Stressed liquid crystals (SLCs) have been applied in fields such as optical phase array non-mechanical beam steering applications, adaptive optical tip-tilt correction, and fast displays because SLCs are capable of switching large phase shift in sub-millisecond time ranges. SLCs consist of liquid crystal micro-domains dispersed in a stressed polymer matrix. In this paper, we propose a model of close-packed, shaped liquid crystal droplets inside a sheared polymer matrix based upon the measurements of polarizing microscopy, fluorescence confocal microscopy, and visible-near-infrared spectroscopy. The light scattering of SLC films results mostly from the index mismatch between adjacent liquid crystal domains instead of the index mismatch between polymer matrices and liquid crystals as in traditional polymer dispersed liquid crystals. We show how the light scattering of SLC cells is greatly reduced upon shearing because the liquid crystal domains are aligned along the direction of shearing. The stretching of polymer matrices and the reshaping of liquid crystal domains upon shearing are confirmed by fluorescence confocal microscopy. The calculations of the electro-optic responses are based on the balance between the elastic torque and the electric field torque. Our experimental results support the calculations.

Keywords: liquid crystal, polymer, stress, model, fluorescence confocal microscopy, light scattering, electro-optic performance

1. INTRODUCTION

Polymer/liquid-crystal composites are promising light modulating materials for displays, shutters, switchable windows, etc. Many methods have been used to construct fast switching polymer/liquid-crystal composites, such as polymer stabilized liquid crystal (PSLC[1]), holographic polymer dispersed liquid crystal (HPDLC[2]), and polymer network liquid crystal (PNLC[3]). However, a polymer/liquid-crystal composite providing large phase shift with fast switching speed while maintaining optimum optical properties is still under development. Introducing stress to polymer/liquid-crystal composites[4,5,6] leads to the appearance of special features, such as shear-induced orientation, light polarization, and fast response. When a traditional polymer dispersed liquid crystal (PDLC) is stretched[7], it becomes a polarizer, transmitting light with polarization perpendicular to the stretching direction and scattering light with polarization parallel to the stretching direction. However, unlike stretched PDLCs, stressed liquid crystals[8,9] (SLCs) do not scatter with a

* johnwest@lci.kent.edu ; website: www.lci.kent.edu/westlab

Liquid Crystals IX, edited by Iam-Choon Khoo, Proceedings of SPIE Vol. 5936
(SPIE, Bellingham, WA, 2005) · 0277-786X/05/$15 · doi: 10.1117/12.618358

polarization anisotropy, rather light of any of both polarizations is transmitted. SLCs are comprised of interconnected micro-domains of a liquid crystal dispersed in a stressed polymer matrix. There are three major benefits of applying shearing stress in an SLC system: 1) liquid crystal alignment along the shearing direction substantially reduces light scattering and increases phase shift; 2) greatly reduces response times; 3) produces a linear response between phase shift and applied voltage. In an SLC system, uniform shear-induced orientation of a liquid crystal can be maintained in a cell thicker than 500 μm. Therefore, large phase shift (i.e., greater than 30 μm) can be obtained from a single SLC sample. As a result of switching large birefringence in the sub-millisecond range, SLCs have been utilized in areas such as optical phase array[10] non-mechanical beam steering applications[11], adaptive optical tip-tilt correction and fast displays.

In this paper, we study SLCs of different domain sizes, ranging from sub-micron to over 30 microns, by optical microscopy, fluorescence confocal microscopy[12], and Vis-NIR spectroscopy. We propose a simplified model of close-packed, shaped liquid crystal droplets inside a sheared polymer matrix for the SLC system. Based on the balance of the elastic torque and the electrical torque, we calculate the switching fields and response times for a 40-micron-thick SLC sample of sub-micron domains. We then compare the calculation results with the experimental electro-optic measurements.

2. EXPERIMENTS

The liquid crystal material we used is a cyanobiphenyl liquid crystal from Merck: 4-pentyl-4'-cyanobiphenyl (5CB). The monomers are NOA65, from Norland Optical Adhesive, Inc. and RM82, a reactive mesogen diacrylate monomer from Merck.

We first mixed 5CB, RM82 and NOA65 at a weight ratio of 94:2:4. The initiator (Irgacure) is 0.1 percent of the whole mixture in weight. Then we sandwiched the mixture between two indium-tin-oxide (ITO) coated glasses with 12 μm fiber spacers to control the cell thickness. No alignment layers were applied. Next, we polymerized these samples at 60^{o}C for 20 minutes under UV exposure before cooling them to room temperature at different cooling rates. An additional 20 minutes' post-cure at a UV intensity of 22mW/cm^2 was applied at 20^{o}C to guarantee complete polymerization. In addition, we fabricated a 40 micron-thick SLC sample (5CB-5) of sub-micron domains using a mixture at a weight ratio of 90:2:8 (5CB:RM82:NOA65). The electro-optic properties were measured and compared with our calculations later on (fabrication conditions tabulated in Table 1).

Once we prepared the 5CB-SLC samples, we characterized the shearing-distance-dependent transmittance. In addition, 5CB-2 and 5CB-3 with relatively large liquid crystal domains (5 to 20 μm) were selected to study the shearing deformation of polymer matrix using polarizing microscopy and fluorescence confocal microscopy. As for the fluorescence confocal microscopic measurements, we selected a fluorescent dye that accumulates in the polymer matrix during polymerization, enhancing the contrast. The concentration of dye was minimal, 10^{-4} by weight. Very thin (i.e., ~0.1 mm) ITO-glass substrates were used as the top substrates. The image data were collected by scanning the tightly

focused laser beam in the vertical cross-section of the sample, providing side views of the polymer morphology between the two bounding plates.

During electro-optic measurements, we placed the SLC samples in between two crossed polarizers. The shearing direction was aligned at a 45° angle to each polarizer. The laser wavelength was 633 nm. A continuous ramp of voltages was applied to measure switching fields at each shearing distance. At a specific voltage value, liquid crystals were completely switched so that the transmitted light intensity would be at its minimum and would not change with an increase of voltage. We recorded that voltage value as the switching voltage. The switching field was calculated as E = V/d, where d is the thickness of an SLC sample. The rise time (τ_{on}) measures a time period for liquid crystals to be completely oriented along the switching field from the initial unpowered state to the powered state. On the other hand, to measure relaxation time (τ_{off}), we first applied a switching electric field to align liquid crystals along the field direction. We then removed the field to allow the liquid crystals to relax back to their initial unpowered state. The time that liquid crystals take to relax back is τ_{off}.

3. RESULTS AND DISCUSSIONS

In Table 1, we show the fabrication conditions for the five 5CB-SLC samples and the estimation of the liquid crystal domain sizes. Low UV intensity cure allows slower polymerization, therefore producing larger liquid crystal domains. In addition, slow cooling favors coalescence of liquid crystal domains, which gives rise to large droplets as well. The droplet sizes were estimated from the micrographs shown in Fig. 1, except for sample 5CB-5, for which the size was obtained from scanning electron microscopic pictures (not included).

Table 1: Fabrication conditions of the four 5CB-SLC samples with different sizes of liquid crystal domains

5CB-SLC Samples	5CB-1	5CB-2	5CB-3	5CB-4	5CB-5
Cell gap (μm)	12	12	12	12	40
Composition 5CB/RM82/NOA65	94:2:4	94:2:4	94:2:4	94:2:4	90:2:8
UV intensity (mW/cm^2)	6.0	6.0	22	40	40
Cooling rate (°C/min)	0.4	4	4	4	4
Liquid crystal domain size: D_{LC} (diameter in μm)	30-40	10-20	5-8	~2	0.2~0.5 (observed from SEM)

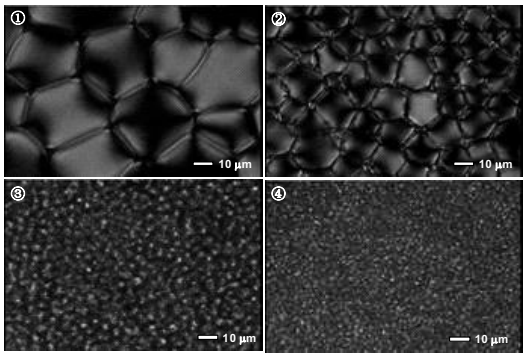

Figure 1: Micrographs of 5CB-SLC samples made of 5CB/ RM82/ NOA65 (94:2:4): 5CB-1 to 5CB-4, with different sizes of liquid crystal domains. The white bar represents 10 μm in length scale.

Inside an SLC, each liquid crystal domain is surrounded by other randomly-oriented liquid crystal domains separated by polymer sheets. The major cause of light scattering is the refractive index mismatch between adjacent liquid crystal domains. The light scattering also results from the refractive index mismatch between the liquid crystal and the polymer matrix. However, the mismatch is less significant because the dimension of a polymer sheet is much smaller than that of a liquid crystal domain[13,14]. The mismatch of the refractive index between liquid crystal domains disappears when liquid crystal domains are aligned in the same direction upon shearing. Thus, the light scattering of the film is reduced drastically.

The transparency of SLCs depends significantly on the fabrication conditions, such as UV intensity and curing temperature. We examined the transmittance of the five 5CB-SLC samples at two states: before-shearing and after-shearing. At the after-shearing state, we measured the spectra at the saturation point of shearing, beyond which further shearing will not reduce light scattering any more. The reference used to correct reflection loss is a fully-cured 12-μm-thick NOA65 film sandwiched between two ITO glasses. We use a parameter R_{shear} to represent the shearing ability: $R_{shear} = L_{MAX}/d$, where L_{MAX} is the maximum shearing distance beyond which an SLC film will be broken and d is the thickness of an SLC film. We found that there is little difference (Fig. 2a) between the states of before-shearing and after-shearing for the samples 5CB-1 and 5CB-2. This is due to the less shearing ability of these two samples: $R_{shear} < 4$ (L_{MAX} is less than 40 μm while d is 12 μm). In contrast, shearing has a greater influence on the samples 5CB-3, 5CB-4, and 5CB-5 as seen in Fig. 2b. In particular, the sample 5CB-5, with the smallest of the liquid crystal domains, shows the best shearing ability ($R_{shear} > 8$) and the most significant increase of transmission at the after-shearing state. There is essentially no light scattering at the near infrared region.

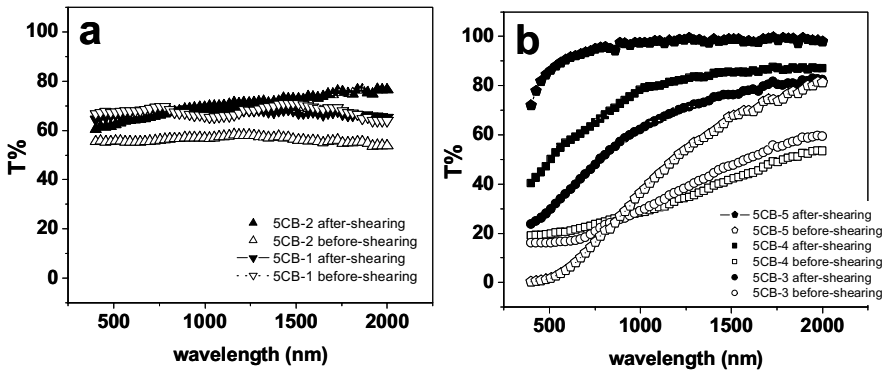

Figure 2: Transmittance of 5CB-SLC samples of different sizes of liquid crystal domains at the states of before- and after-shearing: a) 5CB-1 and 5CB-2; b) 5CB-3, 5CB-4, and 5CB-5. The hollow and solid symbols represent before-shearing and after-shearing states, respectively.

To study the shearing deformation, we selected the two samples with relatively large liquid crystal domains, 5CB-2 (10 to 20 μm in diameter) and 5CB-3 (5 to 10 μm in diameter). Fig. 3 displays microscopic top-views of these two samples. The dark lines indicate a polymer matrix while the light regions indicate liquid crystals confined between the polymer sheets. Comparing the before-shearing and the after-shearing states of the sample 5CB-3 (Fig. 3a and 3b), we see that, along the shearing direction, dark lines became parallel to each other, demonstrating that polymer matrices are stretched during shearing. Liquid crystal domains formed a polygonal droplet shape before shearing for sample 5CB-2 (Fig. 3c). After shearing, the liquid crystal domains were elongated as seen in Fig. 3d. Therefore, we observed two major shearing effects on SLCs' structures: the stretch of polymer matrices and the elongation of liquid crystal domains.

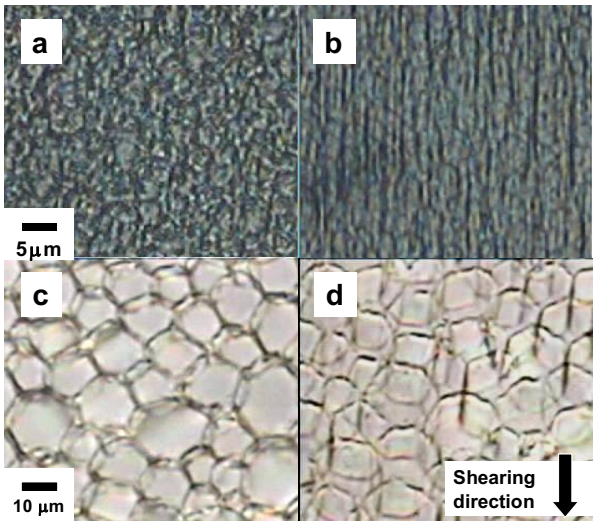

Figure 3: Microscopic pictures of samples 5CB-2 (c,d) and 5CB-3 (a,b): (a), (c) the before-shearing state; (b), (d) the after-shearing state. The horizontal black bars represent length scales for the two samples. The shearing direction is depicted by the dark arrow.

Fluorescence confocal micrographs confirmed the two shearing effects. Fig. 4 shows fluorescence confocal microscopic textures of the vertical optical scans of samples 5CB-2 and 5CB-3. The image data are collected by scanning the tightly focused laser beam in the vertical cross-section of the sample, providing the side view of the polymer morphology between the two bounding plates; the plates are seen as dark top and bottom regions in Fig. 4. Fig. 4a and 4b were taken before shearing samples 5CB-2 and 5CB-3, while Fig. 4c and 4d were taken after shearing. The shearing direction is from left to right. The white color represents the polymer matrix whereas the gray color inside the white is the liquid crystal domain. One can see that, during shearing, polymer matrices in both SLC samples are stretched along the direction of shearing and liquid crystal domains adopt an elongated shape.

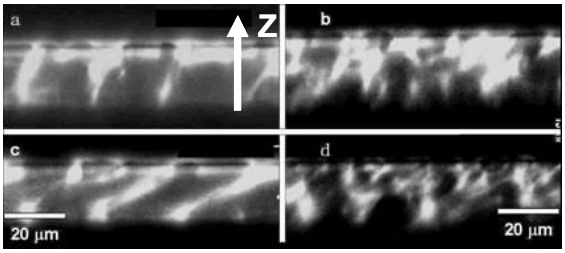

Figure 4: Fluorescence confocal microscopic Z-scan pictures of samples 5CB-2 and 5CB-3 before and after shearing. a) before-shearing of 5CB-2; b) before-shearing of 5CB-3; c) after-shearing of 5CB-2; d) after-shearing of 5CB-3.

4. THE MODEL

Based on the microscopic studies, we propose a simplified model of stressed liquid crystals: close-packed, shaped liquid crystal droplets inside a sheared polymer matrix. In this model, SLCs are composed of multiple stacks of liquid crystal hexagonal tubes separated by thin polymer sheets. The model is illustrated in Fig. 5. Both the side view and the top view are presented in order to demonstrate the shearing mechanism.

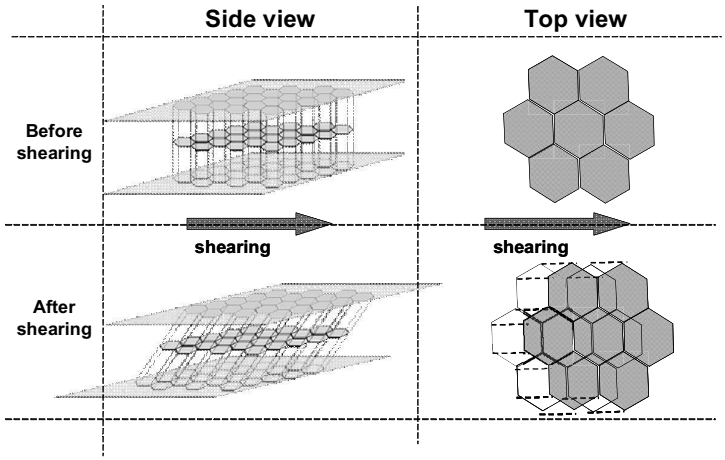

Figure 5: The model of shearing close-packed, shaped liquid crystal domains: including the side view and the top view.

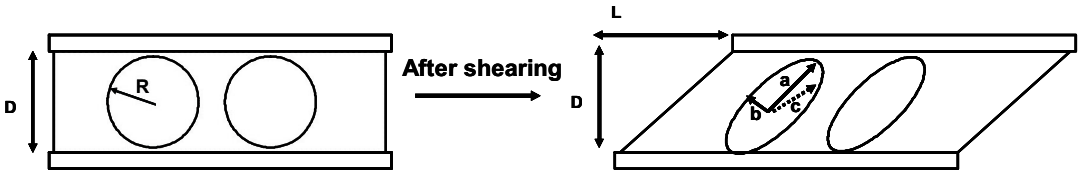

Figure 6: Deformation of liquid crystal droplets during shearing. L is the shearing distance; D is the cell thickness; R is the radius of original spherical droplet. A, b, and c represent semi-major axis, semi-minor axis at the direction along shearing direction, and semi-minor axis at the direction perpendicular to shearing direction, respectively.

First, we simplified the hexagonal tubes into spherical droplets in the before-shearing state and ellipsoids in the after-shearing state. Then we neglected the interaction between adjacent droplets to calculate electro-optic properties. Modified from B-G Wu's model[4], we derived formulas for switching electrical fields and response times of an SLC system at different shearing distances. As depicted in Fig. 6, geometrically, the semi-major axis can be obtained as $a = R^*\sqrt{(\frac{L}{d})^2+1} = R^*\sqrt{(L_1)^2+1}$ where $L_1 = L/d$. We assumed that the volume of liquid crystal droplets does not change during shearing. Thus, we have $a^*b^*c = R^3$. From the microscopic study, we assumed $c = R$ (the width of droplet does not change as shown in Fig. 3d). Thus, we derived b as $b = R^2/a = R/\sqrt{(L_1)^2+1}$. Then the aspect ratio (l) is calculated as: $l = \frac{a}{b} = (L_1)^2+1$. Therefore, the formulas for response times and switching voltage are listed as follows:

Relaxation time (τ_{off}):

$$\tau_{off} = \frac{\gamma a^2}{K(l^2-1)} = \frac{\gamma R^2\left(L_1^{\,2}+1\right)}{K\left(\left(L_1^{\,2}+1\right)^2-1\right)} \tag{1}$$

where γ is the rotational viscosity of a liquid crystal, a is the long axis of a liquid crystal droplet, K_{33} is the bend elastic constant of a liquid crystal, and l is the aspect ratio, $l = \frac{a}{b}$, where b is the short axis of a liquid crystal droplet.

Rise time (τ_{on}):

$$\tau_{on} = \frac{\gamma}{\sqrt{\left(\frac{K_{33}\left(\left(L_1^{\,2}+1\right)^2-1\right)}{R^2\left(L_1^{\,2}+1\right)}+\Delta\varepsilon E^2\right)^2+\left(\frac{K_{33}\left(\left(L_1^{\,2}+1\right)^2-1\right)}{R^2\left(L_1^{\,2}+1\right)}\right)\cdot\left(\Delta\varepsilon E^2\right)\cdot\left(\frac{4}{\left(L_1^{\,2}+1\right)}-4\right)}} \tag{2}$$

where $\Delta\varepsilon$ is the dielectric anisotropy of a liquid crystal and E is the strength of an applied electric field.

Switching field (E_{switch}):

$$E_{switch} = \frac{V_{switch}}{d} = \frac{1}{3a}\left(\frac{\sigma_2}{\sigma_1}+2\right)\left(\frac{K_{33}\left(l^2-1\right)}{\Delta\varepsilon}\right)^{\frac{1}{2}} = \frac{1}{3R\sqrt{L_1^{\,2}+1}}\left(\frac{\sigma_2}{\sigma_1}+2\right)\left(\frac{K_{33}\left((L_1^{\,2}+1)^2-1\right)}{\Delta\varepsilon}\right)^{\frac{1}{2}} \tag{3}$$

where σ_1 and σ_2 are the conductivities of a polymer matrix and a liquid crystal, respectively.

We calculated the electro-optic responses of the SLC sample 5CB-5, and compared the calculations with our experimental results. The data for the calculation parameters are tabulated in Table 2. According to SEM micrographs, the liquid crystal domain size is in the range of 0.2 ~ 0.5 μm. Therefore, we selected two radius R_1=0.2 μm and R_2 =0.5 μm to calculate the electro-optic responses. The results are compared in Fig. 7.

Table 2: Parameters used in the calculations.

γ (kg/ms)	σ_2/σ_1	K_{33} (10^{-11} N)	Δε	R_1 (μm)	R_2 (μm)
0.056	20	0.61	12	0.2	0.5

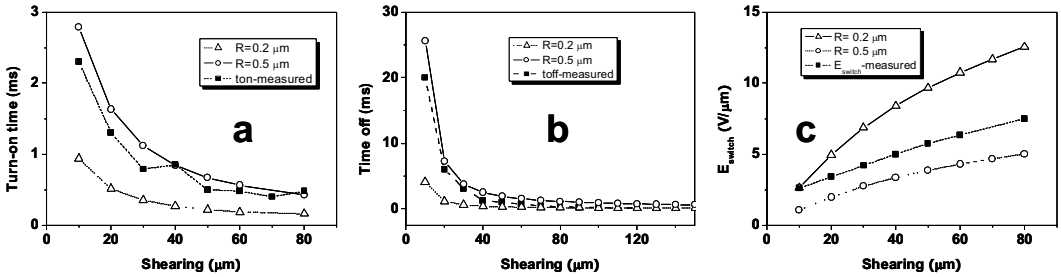

Figure 7: Comparison between calculations and experimental measurements: a) turn-on time; b) relaxation time; c) switching field. The hollow triangles with dotted lines represent the calculation results using R_1=0.2 μm; the hollow circles with dashed lines represent the calculation results using R_1=0.5 μm; the solid squares with solid lines represent the experimental data.

As seen in all three graphs of Fig. 7, the experimental curves agree well with the two corresponding calculated curves. The switching field increases with the increase of the shearing distance. In addition, both the relaxation time and the rise time decrease with the increase of the shearing distance. As such, this model provides a useful tool to predict electro-optic performance of SLCs.

5. CONCLUSIONS

We propose a simplified model of stressed liquid crystals: close-packed, shaped liquid crystal droplets inside a sheared polymer matrix. We investigated the shearing effects in the stressed liquid crystal system, such as variations of light scattering and changes of electro-optic properties upon shearing. The experimental data are in good agreement with the calculation results. Future research may take into account the interconnection of adjacent liquid crystal droplets and other relevant factors to enrich this model. All in all, our model sheds light on the mechanism of stressed liquid crystals and helps to optimize this system.

ACKNOWLEDGMENTS

This research is partially funded under DARPA grant # 444266.

REFERENCES

1 Y. K. Fung, A. Borstnik, S. Zumer, D.-K. Yang et al., "Pretransitional nematic ordering in liquid crystals with dispersed polymer networks," Phys. Rev. E 55 (2), 1637-1645 (1996).

2 Timothy J. Bunning, Lalgudi V. Natarajan, Vincent P. Tondiglia, and R. L. Sutherland, "Holographic Polymer-Dispersed Liquid Crystals (H-PDLCs)," Annu. Rev. Mater. Sci. 30, 83-115 (2000).

3 Yun-Hsing Fan, Hongwen Ren, Xiao Liang, Yi-Hsin Lin et al., "Dual-frequency liquid crystal gels with submillisecond response time," Appl. Phys. Lett. 85 (13), 2451-2453 (2004).

4 Bao-Gang Wu, John H. Erdmann, and J. William Doane, "Response times and voltages for PDLC light shutters," Mol. Cryst. Liq. Cryst. 5 (5), 1453 (1989).

5 Heinz-S. Kitzerow, Henning Molsen, and Gerd Heppke, "Linear electro-optic effects in polymer-dispersed ferroelectric liquid crystals," Appl. Phys. Lett. 60 (25), 3093-3095 (1992).

6 C. M. Leader, W. Zheng, J. Tipping, and H. J. Coles, "Shear aligned polymer dispersed ferroelectric liquid crystal devices," Liq. Cryst. 19 (4), 415-419 (1995).

7 Ichiro Amimori, Nikolai V. Priezjev, Robert A. Pelcovits, and Gregory P. Crawford, "Optomechanical properties of stretched polymer dispersed liquid crystal films for scattering polarizer applications," J. Appl. Phys. 93 (6), 3248-3252 (2003).

8 John L. West, Guoqiang Zhang, and Anatoliy Glushchenko, "Stressed Liquid Crystals for Electrically Controlled Fast Shift of Phase Retardation," SID tech Digest 55-1 (2003).

9 John L. West, Guoqiang Zhang, Anatoliy Glushchenko, and Yurii Reznikov, "Fast birefringent mode stressed liquid crystal," Appl. Phys. Lett. 86 (3), 031111 (2005).

10 Paul F. McManamon, Terry A. Dorschner, David L. Corkum, Larry J. Friedman et al., "Optical Phased Array Technology," *Proc. IEEE 84* (2), 268-298 (1996).

11 John L. West, Guoqiang Zhang, Ke Zhang, and Anatoliy Glushchenko, "Stressed Liquid Crystals for Fast Beam Steering Devices," Liquid Crystal Conference, Great Lakes Photonics Symposium, Cleveland, OH (2004).

12 I. I. Smalyukh, S. V. Shiyanovskii, and O. D. Lavrentovich, "Three-dimensional imaging of orientational order by fluorescence confocal polarizing microscopy," Chemical Physics Letters 336 (1-2), 88-96 (2001).

13 Paul S Drzaic, "Droplet density, droplet size, and wavelength effects in PDLC light scattering," Mol. Cryst. Liq. Cryst. 261, 383-392 (1995).

14 Karl Amundson, Alfons van Blaaderen, and Pierre Wiltzius, "Morphology and electro-optic properties of polymer-dispersed liquid-crystal films," Phys. Rev. E 55 (2), 1646- (1997).